Thick optical waveguides in lithium niobate induced by swift heavy ions (10 MeV/amu) at ultralow fluences

J. Olivares, M.L. Crespillo, O. Caballero-Calero, M.D. Ynsa, A. Garcia-Cabanes, Marcel Toulemonde, C. Trautmann, F. Agullo-Lopez

Thick optical waveguides in lithium niobate induced by swift heavy ions (~10 MeV/amu) at ultralow fluences

José Olivares,[1,2,*] Miguel L. Crespillo,[2] Olga Caballero-Calero,[2,3] María D. Ynsa,[2] Angel García-Cabañes,[4] Marcel Toulemonde,[5] Christina Trautmann,[6] and Fernando Agulló-López[2]

[1]*Instituto de Optica, Consejo Superior de Investigaciones Científicas, C/Serrano 121, 28016-Madrid, Spain.*
[2]*Centro de Microanálisis de Materiales (CMAM), Universidad Autónoma de Madrid, 28049-Madrid, Spain.*
[3]*Currently with the Laboratoire d'Astrophysique de Grenoble, 38400 Grenoble, France.*
[4]*Depto. de Física de Materiales, Facultad de Ciencias, Universidad Autónoma de Madrid, 28049-Madrid, Spain.*
[5]*Laboratoire CIMAP-GANIL, Bd H. Becquerel, BP 5133, 14070 CAEN-cedex 05, France.*
[6]*Gesellschaft für Schwerionenforschung (GSI), Materialforschung, Planckstr. 1, 64291 Darmstadt, Germany*
*j.olivares@io.cfmac.csic.es

Abstract: Heavy mass ions, Kr and Xe, having energies in the ~10 MeV/amu range have been used to produce thick planar optical waveguides at the surface of lithium niobate ($LiNbO_3$). The waveguides have a thickness of 40-50 micrometers, depending on ion energy and fluence, smooth profiles and refractive index jumps up to 0.04 (λ = 633 nm). They propagate ordinary and extraordinary modes with low losses keeping a high nonlinear optical response (SHG) that makes them useful for many applications. Complementary RBS/C data provide consistent values for the partial amorphization and refractive index change at the surface. The proposed method is based on ion-induced damage caused by electronic excitation and essentially differs from the usual implantation technique using light ions (H and He) of MeV energies. It implies the generation of a buried low-index layer (acting as optical barrier), made up of amorphous nanotracks embedded into the crystalline lithium niobate crystal. An effective dielectric medium approach is developed to describe the index profiles of the waveguides. This first test demonstration could be extended to other crystalline materials and could be of great usefulness for mid-infrared applications.

OCIS codes: (130.3120) Integrated optics devices; (130.2790) Guided waves; (130.3730) Lithium niobate;

References and links

1. P. D. Townsend, P. J. Chandler, and L. Zhang, *Optical Effects of Ion Implantation* (Cambridge University Press, Cambridge, 1994).
2. F. Chen, X.-L. Wang, and K.-M. Wang, "Development of ion-implanted optical waveguides in optical materials: A review," Opt. Mater. **29**(11), 1523–1542 (2007).
3. F. Chen, "Photonic guiding structures in lithium niobate crystals produced by energetic ion beams," J. Appl. Phys. **106**(8), 081101 (2009).
4. J. Olivares, G. Garcia, A. Garcia-Navarro, F. Agulló-López, O. Caballero, and A. Garcia-Cabañes, "Generation of high-confinement step-like optical waveguides in $LiNbO_3$ by swift ion-beam irradiation," Appl. Phys. Lett. **86**(18), 183501 (2005).
5. G. G. Bentini, M. Bianconi, M. Chiarini, L. Correa, C. Sada, P. Mazzoldi, N. Argiolas, M. Bazzan, and R. Guzzi, "Effect of low dose high energy O3+ implantation on refractive index and linear electro-optic properties in X-cut LiNbO3: Planar optical waveguide formation and characterization," J. Appl. Phys. **92**(11), 6477 (2002).
6. J. Olivares, A. García-Navarro, G. García, F. Agulló-López, F. Agulló-Rueda, A. García-Cabañes, and M. Carrascosa, "Buried amorphous layers by electronic excitation in ion-beam irradiated lithium niobate: structure and kinetics," J. Appl. Phys. **101**(3), 033512 (2007).
7. M. Bianconi, N. Argiolas, M. Bazzan, G. G. Bentini, M. Chiarini, A. Cerutti, P. Mazzoldi, G. Pennestri, and C. Sada, "On the dynamics of the damage growth in 5 MeV oxygen-implanted lithium niobate," Appl. Phys. Lett. **87**(7), 072901 (2005).

#118545 - $15.00 USD Received 13 Oct 2009; revised 30 Nov 2009; accepted 30 Nov 2009; published 18 Dec 2009

8. A. Rivera, J. Olivares, G. García, J. M. Cabrera, F. Agulló-Rueda, and F. Agulló-López, "Giant enhancement of material damage associated to electronic excitation during ion irradiation: The case of $LiNbO_3$," Phys. Status Solidi A **206**(6), 1109–1116 (2009).
9. M. Toulemonde, C. Trautmann, E. Balanzat, K. Horjt, and A. Weidinger, "Track formation and fabrication of nanostructures with MeV-ion beams," Nucl. Instr. Meth. B **216**, 1–8 (2004).
10. B. Canut, S. M. M. Ramos, R. Brenier, P. Thevenard, J. L. Loubet, and M. Toulemonde, "Surface modification of $LiNbO_3$ single crystals by swift heavy ions," Nucl. Instrum. Methods B **107**(1-4), 194–198 (1996).
11. A. Meftah, F. Brisard, J. M. Constantini, M. Hage-Ali, J. P. Stoquert, F. Studer, and M. Toulemonde, "Swift heavy ions in magnetic insulators: a damage cross-section velocity effect," Phys. Rev. B **48**(2), 920–925 (1993).
12. A. Meftah, J. M. Constantini, N. Khalfaoui, S. Boudjadar, J. P. Stoquert, F. Studer, and M. Toulemonde, "Experimental determination of track cross-section in GdGaO and comparison to the inelastic thermal spike model applied to several materials," Nucl. Instrum. Methods B **237**(3-4), 563–574 (2005).
13. A. Majkic, M. Koechlin, G. Poberaj, and P. Günter, "Optical microring resonators in fluorine-implanted lithium niobate," Opt. Express **16**, 8769 (2008).
14. J. Olivares, A. García-Navarro, G. García, A. Méndez, and F. Agulló-López, "Optical determination of 3-D nano-track profiles generated by single swift-heavy ion impacts in $LiNbO_3$," Appl. Phys. Lett. **89**, 71923 (2006).
15. A. García-Navarro, J. Olivares, G. García, F. Agulló-López, S. García-Blanco, C. Merchant, and J. Stewart Aitchison, "Fabrication of optical waveguides in KGW by swift heavy ion beam irradiation," Nucl. Instrum. Meth. B **249**(1-2), 177–180 (2006).
16. C. A. Merchant, P. Scrutton, S. García-Blanco, C. Hnatovsky, R. S. Taylor, A. García-Navarro, G. García, F. Agulló-López, J. Olivares, A. S. Helmy, and J. S. Aitchison, "High-Resolution Refractive Index and Micro-Raman Spectroscopy of Planar Waveguides in $KGd(WO_4)_2$ formed by Swift Heavy Ion Irradiation," IEEE J. Quantum Electron. **45**(4), 373–379 (2009).
17. J. Bland-Hawthorn, and P. Kern, "Astrophotonics: a new era for astronomical instruments," Opt. Express **17**(3), 1880–1884 (2009).
18. L. Labadie, and O. Wallner, "Mid-infrared guided optics: a perspective for astronomical instruments," Opt. Express **17**(3), 1947–1962 (2009).
19. *The Stopping and Ranges of Ions in Solids*, edited by J.F. Ziegler, J.P. Biersack and U. Littmark (Pergamon Press, New York, 1985); see also the SRIM web page http://www.srim.org.
20. K. S. Chiang, "Construction of refractive-index profiles of planar dielectric waveguides from distribution of effective indexes," J. Lightwave Technol. **3**(2), 385–391 (1985).
21. P. Thévenard, G. Guiraud, C. H. S. Dupuy, and B. Delaunay, "Assumption of F-centre creation in lif bombarded with high-energy particles," Radiat. Eff. **32**(1), 83–90 (1977).
22. J. Rams, and J. M. Cabrera, "Second harmonic generation in the strong absorption regime," J. Mod. Opt. **47**(10), 1659–1669 (2000).
23. M. Toulemonde, C. Dufour, and E. Paumier, "Transient thermal process after a high-energy heavy-ion irradiation of amorphous metals and semiconductors," Phys. Rev. B **46**(22), 14362–14369 (1992).
24. O. Caballero-Calero, M. Kösters, T. Woike, K. Buse, A. García-Cabañes, and M. Carrascosa, "Electric field periodical poling of lithium niobate crystals after soft-proton-exchanged," Appl. Phys. B **88**(1), 75–78 (2007).
25. O. Caballero-Calero, A. García-Cabañes, M. Carrascosa, F. Agulló-López, J. Villarroel, M. Crespillo, and J. Olivares, "Periodic poling of optical waveguides produced by swift-heavy ion irradiation in $LiNbO_3$," Appl. Phys. B **95**(3), 435–439 (2009).
26. G. García, J. Olivares, F. Agulló-López, A. García-Navarro, F. Agulló-Rueda, A. García-Cabañes, and M. Carrascosa, "Effect of local rotations on the optical response of $LiNbO_3$: application to ion-beam damage," Europhys. Lett. **76**(6), 1123–1129 (2006).

1. Introduction

Ion implantation of light ions (H or He) in the few-MeV energy range is a standard procedure to produce optical waveguides at visible and near-IR wavelengths in $LiNbO_3$ and in many other crystals [1–3]. At the end of their range (~1 μm), ions are implanted and severe structural damage is produced by elastic collisions with the atoms of the target material, leading to the formation of a buried layer having a lower density and refractive index than the virgin crystal. This buried layer behaves as an optical barrier creating a surface waveguide. For the formation of such a barrier fluences as high as 10^{16}-10^{17} ions/cm^2 are required. At the typical currents obtained in ion accelerators the method becomes quite inefficient. The fact that the thickness of the optical barrier produced with MeV ions is limited to about 1 micron does not allow for full infrared light confinement. Propagation losses thus increase due to light tunnelling to the substrate modes (i.e. leaky modes). This problem could be overcome by using ions of larger energy and thus large range leading to thicker layers of modified material.

Recently this method has been tested for $LiNbO_3$ demonstrating not only the feasability but also a number of advantages such as substancially reduced ion fluences [4]. The irradiation requires heavier projectiles (mass in the range 15 to 40 atomic units), and energies in the range of a few tens of MeV. For such high energies, the electronic energy deposition is

#118545 - $15.00 USD Received 13 Oct 2009; revised 30 Nov 2009; accepted 30 Nov 2009; published 18 Dec 2009

dominant and responsible for structural modifications of the material [4–7]. The damage induced in the electronic energy loss regime has quite different features compared to defects produced by elastic collisions [8]. Track formation, i.e., the formation of columnar defects requires a well-defined electronic stopping power threshold value, and, on $LiNbO_3$, the damage cross-section of the tracks strongly increases with the energy loss, dE/dx. By analogy with the track morphology as depicted in the reference [9], it is possible to define specific thresholds versus electronic energy loss [10] taking into account the velocity effect [11]. At low velocity (~0.1 MeV/amu) threshold of damage creation is ~2 keV/nm and threshold of continuous track is ~7.5 keV/nm while at high energy (10 MeV/amu) the corresponding thresholds are ~6.5 and ~13 keV/nm, respectively. In between these two thresholds the damage in the track is inhomogeneous and not continuous. However, by accumulating high fluences homogeneous amorphous layers can be created due to track overlapping.

The idea behind the fabrication of an optical waveguide with high-energy ions is to bombard the material with ions having their electronic energy loss maximum at a certain depth inside the material. At and around this maximum, the damage threshold can be overcome producing an amorphous layer of lower refractive index. This buried layer constitutes an optical barrier for waveguiding at the surface. In first test experiments, $LiNbO_3$ was bombarded with F ions of 22 MeV energy and maximum stopping power of about 3 keV/nm (i.e. below the threshold of continuous track damage). The irradiation produced useful waveguides with high refractive index jump (~10%), step-like index profile (due to track overlapping) with low propagation losses and reasonably high nonlinear optical coefficients. The applied fluences were around 10^{14} cm^{-2}, which is compared to standard low-energy implantation, reduced by two orders of magnitude [4]. Following the same technique, lithium niobate ring resonators with 80 μm radius acting as wavelength filters at the 1.5 μm telecom wavelength have been fabricated [13]. In a later work, waveguides having an heterogeneous structure were achieved with heavier ions of MeV energy such as Cl ions of about 7 keV/nm energy loss which is above the amorphisation threshold. To prevent full surface amorphization, the irradiation was performed with isolated, i.e. non-overlapping tracks corresponding to fluences as low as 10^{12} - 10^{13} ions/cm^2 [14]. Later on the method was successfully applied to generate optical waveguides in another nonlinear optical crystal, $KGd(WO_4)_2$ [15,16], slightly changing the irradiation conditions. This shows that the method could have a wide applicability to many other crystals with photonic interest.

The purpose of this work has been to explore the use of the heavy ion irradiation method, in the electronic energy loss regime to even higher energies (~10 MeV/amu) and stopping powers. This would allow the fabrication of much thicker waveguides (up to tens of microns) with ultralow fluences (< 10^{12} cm^{-2}). Such thick optical barriers may be useful in the mid-IR e.g. for astrophysical applications (or "Astrophotonics") [17, 18]. Moreover, in this energy range ion trajectories are more straight that would allow for better resolved waveguides patterns. In addition, at such high energies, the contribution of nuclear energy loss is extremely small and defects produced by elastic collisions are irrelevant for the major length of the ion trajectory. Therefore one would expect reduced optical losses after appropriate optimization. Although $LiNbO_3$ is not the most adequate material for applications going beyond 4 microns wavelength due to its large optical absorption, our experiments provide a demonstration test illustrating the potential of the method.

2. Waveguide preparation by swift heavy ion (SHI) irradiation

The irradiations were performed at near normal incidence on Z-cut $LiNbO_3$ samples at GANIL (Caen, France) and GSI (Darmstadt, Germany) with Kr and Xe ions, respectively.

#118545 - $15.00 USD Received 13 Oct 2009; revised 30 Nov 2009; accepted 30 Nov 2009; published 18 Dec 2009

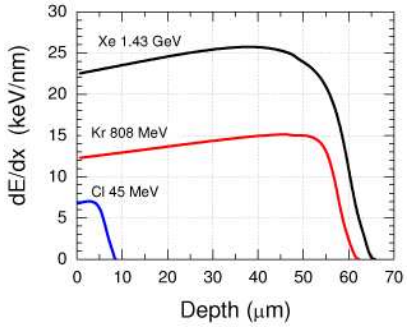

Fig. 1. Electronic energy loss of Kr (809 MeV) and Xe 1432 MeV as a function of penetration depth in $LiNbO_3$ obtained with the SRIM-2003 code [17]. For comparison with earlier experiments [12], the case of Cl (45 MeV) is also shown.

Table 1 lists the corresponding incident energies and ion ranges. Fluences applied ranged from 0.5 up to 8×10^{11} ions/cm^2 . The evolution of the electronic energy loss, calculated with the SRIM-2003 code [19] as a function of penetration depth is shown in Fig. 1. The maximum value is reached at a depth of ~45 μm for Kr (809 MeV) and at ~35 μm for Xe (1450 MeV). In both cases, the energy loss is clearly above the expected amorphisation threshold for a large fraction of the ion trajectory. The figure also includes the curve for 45-MeV Cl ions for comparison with earlier irradiations performed at CMAM (Madrid, Spain) [13].

Table 1. Irradiation parameters including the electronic energy loss S_e at the sample surface and at the Bragg maximum as well as the maximum nuclear energy loss S_n and the projected ion range R_p according to the SRIM-2003 code [19]

Ion	Energy (MeV)	Energy (MeV/amu)	S_e surface (keV/nm)	S_e max (keV/nm)	S_n max (keV/nm)	R_p (μm)
^{78}Kr	809	10.4	12.3	15.1	0.5	62
^{129}Xe	1432	11.1	22.7	25.7	0.9	65

3. Optical characterization: refractive index profiles

$LiNbO_3$ samples irradiated with high-energy Kr or Xe ions (Table 1) indeed show a surface layer that acts as an optical waveguide. This behavior is illustrated in the optical micrographs of Fig. 2 taken from the polished edge of a crystal exposed to 2×10^{11} Xe-ions/cm^2. The irradiated layer (left side) can clearly be seen in the transmission mode, Fig. 2(a), and in the dark-field reflexion mode (R-DF), Fig. 2(b). In the standard bright-field reflexion mode (R-BF, 2c)) only a faint line defines the end of the ion range. The measured thickness of the irradiated layer is ~50 μm which is fair agreement with the ion range predicted by the SRIM-2003 code (cf. Fig. 1).

The surface refractive index profile has been determined by the dark-modes technique at λ = 633 nm. In all cases a quasicontinuum distribution of faint modes was

#118545 - $15.00 USD Received 13 Oct 2009; revised 30 Nov 2009; accepted 30 Nov 2009; published 18 Dec 2009

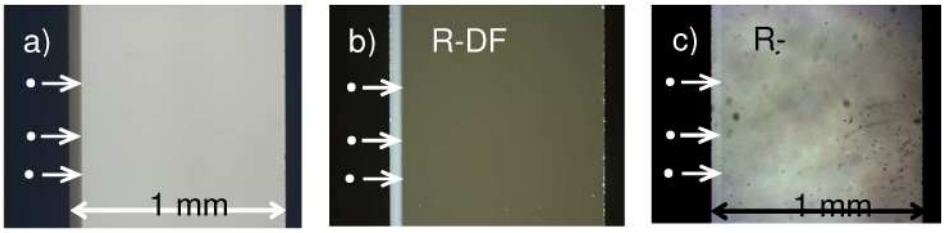

Fig. 2. Optical micrographs from the polished edge of 1-mm thick Z-cut $LiNbO_3$ samples irradiated (from left to right) with Xe ions of fluence $2x10^{11}$ cm^{-2} recorded in (a) transmission mode where the absorbing irradiated layer appears darker, (b) dark-field reflexion mode where the irradiated layer appears brighter than the substrate due to scattering centers, and (c) standard bright-field reflexion mode where a faint line at the depth of the end of ion range appears with different contrast.

observed for the ordinary refractive index. Due to the large thickness of the waveguide the evanescent wave at the surface of the propagating modes for visible wavelength should be quite small decreasing the prism-coupling efficiency. In general, no modes could be observed for the extraordinary polarization with the prism coupling technique (see Discussion), although propagation for both polarizations was possible by end-coupling through the polished edges. For the ordinary polarization we measured the first modes as well as the last mode (i.e. of effective index close to the barrier refractive index). Results for the samples irradiated with Kr ions are shown in Fig. 3, for the the three fluences indicated.

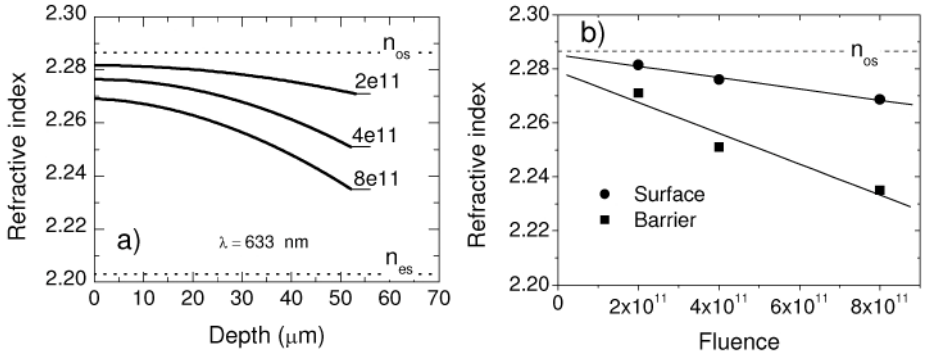

Fig. 3. (a) Refractive index profiles (λ = 633 nm) determined from the dark modes measured for samples irradiated with Kr (809 MeV) at the three fluences indicated in units (ions/cm^2). The substrate refractive indices of $LiNbO_3$ (n_{os} and n_{es}) are shown as dotted lines. (b) Refractive index vs fluence determined at the surface form the index profiles (closed circle) and measured for the optical barrier layer (close squares).

For the fluences $2x10^{11}$ and $4x10^{11}$ ions/cm^2 35 and 43 evenly distributed modes were observed, respectively. With these data a linear function $N_m(m)$ of the mode effective index (N_m) vs mode number (m) was calculated and the refractive index profiles were reconstructed following a standard algorithm based on the Wentzel-Kramer-Brillouin (WKB) approximation valid for smooth index profiles [20]. The sample irradiated with fluence $8x10^{11}$ cm^{-2} broke before having done the mode counting, so its refractive index profile was simply plotted as a proportional one to the one obtained for the fluence $4x10^{11}$ cm^{-2} using the measured surface and barrier refractive indices. The short horizontal lines at the end of each index profile, closed to the label (fluence in ions/cm^2 units), represent the respective refractive indices of the effective substrate and optical barrier, i.e. when continuous light coupling takes place for any angle. The horizontal dotted lines represent the principal refractive indices n_{os} (ordinary) and n_{es} (extraordinary) of the substrate. The refractive index values at the surface and at the barrier as a function of fluence as derived from Fig. 3(a) are shown in Fig. 3(b). For an irradiation with $8x10^{11}$ Kr-ions/cm^2, the overall refractive index jump reaches Δn ~0.04.

#118545 - $15.00 USD Received 13 Oct 2009; revised 30 Nov 2009; accepted 30 Nov 2009; published 18 Dec 2009

For higher fluences, the samples break due to irradiation-induced stress. For fluences below $1x10^{11}$ cm^{-2}, no modes could be observed.

3. Complementary RBS/C data

Rutherford backscattering experiments in a channeling configuration (RBS/C) is a powerful technique to measure the damage or disorder induced near the surface. With He of 2 MeV energy a thickness of about 2 μm can be probed. This information is useful as a cross-check for the optical data and allows for a more complete analysis of the results (see Section 6). Basically, RBS/C data yield the damage fraction f generated at the surface as a function of electronic stopping power S_e and ion fluence ϕ. This fraction is readily derived from the dechanneling yield of an incident beam placed under channeling conditions. Usually, for cylindrical amorphous tracks of radius r, the analysis of the damage fraction versus fluence (Φ) is performed using a Poisson law $f = 1- exp(-\pi r^2 \Phi)$ [21]. In the present experiment and taking into account previous results [12], in the low fluence regime it is possible to make the following approximation $f = \pi r^2 \Phi$ and consequently to deduce the track radius by a linear fit as proposed in the Fig. 4(b). Therefore, RBS/C experiments yield the track radius for any ion and energy.

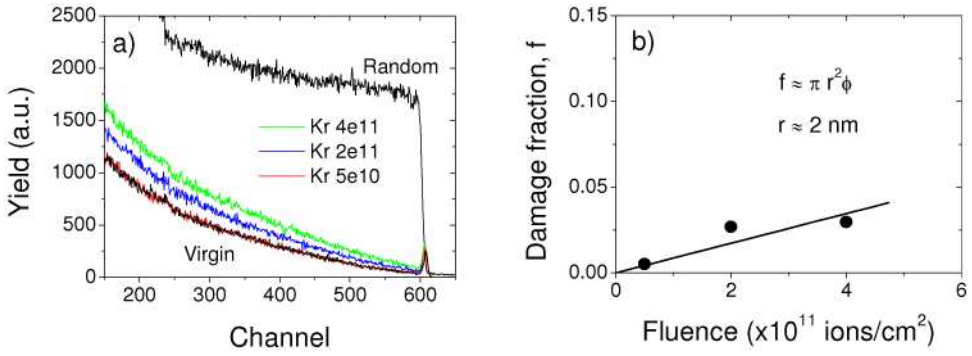

Fig. 4. (a) RBS spectra in channeling and random orientation measured with He (2 MeV) for Z-cut samples irradiated with Kr ions at different fluences; (b) damage fraction (factor f) vs fluence obtained from the RBS/C spectra.

Some complementary RBS/C experiments have been carried out in CMAM (Madrid) in the samples of this work and are shown in the Fig. 4(a) (the Kr case). The damage fraction obtained are shown in Fig. 4(b) and the surface track radius obtained with the analysis indicated is ≈2 nm, close to the literature values.

The radius evolution versus the range, prensented in Fig. 5(a) in the section related to the modelling of the refractive index, is the result of a calculation of track radii using the inelastic thermal spike model developed by Meftah et al. [12] and applied in the present case of Kr irradiation.

4. Linear and nonlinear optical perfomance

Relevant parameters for photonic applications include light propagation losses and second order nonlinear optical coefficients (d_{33} for $LiNbO_3$). Information about propagation losses was obtained by the light scattering method on samples ~2 cm long. Most reliable data for Xe-irradiated samples yield attenuation values in the range 2.6 to 4.5 dB/cm. Prior to this measurement, the samples were annealed in oxygen atmosphere (1 h, at 150 °C) to remove absorption introduced by the ion irradiation. The refractive index profiles and the damage fraction measured by RBS/C remained unchanged after this annealing process. The second harmonic generation (SHG) response has been measured in reflection geometry at a fundamental wavelength of 532 nm by the method described in ref [22]. The relative d_{33} coefficient amounts to 0.5–0.7 of the values for crystalline lithium niobate, and it is not much dependent on fluence, suggesting that light scattering by the amorphous tracks does not

#118545 - $15.00 USD Received 13 Oct 2009; revised 30 Nov 2009; accepted 30 Nov 2009; published 18 Dec 2009

constitute the main mechanism for the losses. For samples irradiated with Xe ions, the coefficient remains at 90% of the unirradiated value. These measured values are lower than expected if we take into account that, according to the RBS/C data, the amorphous fraction at the surface is less than 5%. This could be due to partial ferroelectric domain reversal or depolarization around the amorphous tracks caused either by the strong electronic excitation or the high temperatures reached around each ion tracks [23]. It might be possible in the future to improve this performance by suitable annealing and/or repolarization treatments [24, 25].

5. Discussion: Modeling of the refractive index profiles

Previous experiments have shown that the irradiation of lithium niobate with high energy heavy ions (E > 0.1 MeV/amu) generates along the ion trajectories axially symmetric amorphous tracks. The tracks have a diameter of a few nanometers and are embedded in the crystalline matrix. When the projectile penetrates into the target, the track radius thus first increases due to the increase in energy loss and to the velocity effect (i.e. the amorphization threshold is lower at lower ion velocity) and then decreases once the Bragg maximum has been surpassed. This is, just, the information contained in Fig. 5(a).

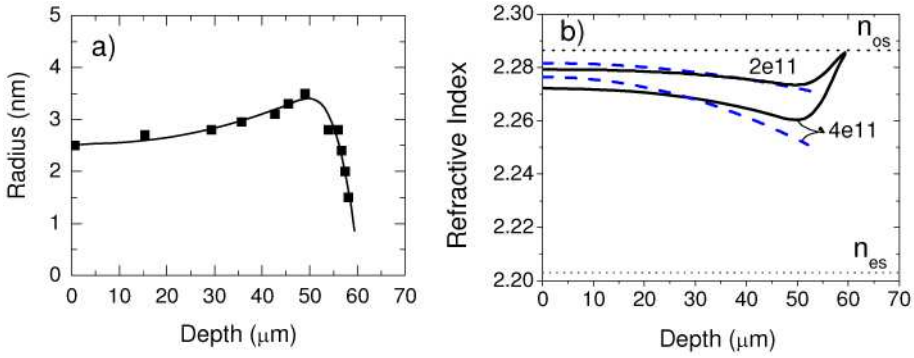

Fig. 5. (a) Track radius vs depth obtained from a calculation using the inelastic thermal spike model developed by Meftah et al. [10] and (b) Theoretical refractive index profiles that would correspond to the track profile shown in (a) for the fluences of $2x10^{11}$ and $4x10^{11}$ cm^{-2}, calculated according to an effective medium approach as discussed in the text. The index profile optically determined for the same fluences are shown (dashed line).

We have then calculated the dependence of refractive index on depth by considering the irradiated $LiNbO_3$ crystal as an effective dielectric medium consisting of the isotropic amorphous tracks (dielectric constant $\varepsilon_a = n_a^2 = 4.41$) and the crystalline matrix (dielectric constant $\varepsilon_o = n_o^2 = 5.23$ (*ordinary*) and $\varepsilon_e = n_e^2 = 4.84$ (*extraordinary*)). It is assumed that the crystalline regions between the well-separated amorphous tracks keep the same refractive indices as the $LiNbO_3$ matrix, i.e., the effects of point defects and mechanical stresses are neglected. Under these conditions the dielectric constant of the effective medium for either ordinary or extraordinary polarization is

$$\bar{\varepsilon}_{e,o} = n_{e,o}^2 = f\,\varepsilon_a + (1-f)\varepsilon_{e,o} \qquad (1)$$

where f ($f = \phi\pi r^2$) is the amorphous fraction, ϕ the ion fluence and r the track radius.

The refractive index profiles derived from this analysis, are shown in Fig. 5(b) for Kr at the fluences of $2x10^{11}$ and $4x10^{11}$ at/cm^2 together with the corresponding profiles optically determined (same as in Fig. 3(a)). The profile calculated from the effective medium is in good agreement with the dark-mode data.

It may be surprising that dark modes have been rarely observed in this work for extraordinary light with the prism-coupling. One possible reason is that, according to the effective medium approach, the change in the refractive index is somewhat higher for the

#118545 - $15.00 USD Received 13 Oct 2009; revised 30 Nov 2009; accepted 30 Nov 2009; published 18 Dec 2009

ordinary index (see Fig. 5). Since this effect is small one can also invoke a more significant but subtle effect. It has been shown that in addition to full amorphization for stopping powers above threshold, irradiation creates isolated defects that also modify the refractive indices [14]. Due to the structure of damage it has been found that even for the non-amorphized crystalline regions the ordinary refractive index experiences a small decrease whereas the extraordinary refractive index increases about twice such decrease in the ordinary index [26]. This will cause a reduction in the overall refractive index of the effective medium balancing or even surpassing the decrease caused by the amorphization. Further work by means of edge-polished micro-reflectance should be performed to clarify this behaviour. Such a detailed study including effects of strain/stress could also help to further improve the matching of the ordinary refractive index profile between the theoretical one and the measured one shown in Fig. 5(b).

Now it becomes clear that a surface layer of modified refractive index can be generated and should be responsible for light waveguiding. Our theoretical argument predicts a refractive index jump quite close to that of the experiment. Another simple and clear prediction, but relevant for the guided infrared applications, is the large thickness of the optical barrier that would provide enough optical confinement, as can be seen in Fig, 5(b).

6. Summary and conclusions

The irradiation with swift heavy-mass ions such as Kr and Xe of energy around 10 MeV/amu and fluences as low as (2-8)x10^{11} cm^{-2} produces thick optical waveguides (~40 μm) keeping a significant fraction of the second-order non-linear optical response and presenting reasonably low propagation losses (~4 dB/cm) in the visible wavelength range. The waveguiding layer is a two-component medium consisting of nanometer-sized amorphous track cylinders aligned perpendicular to the surface and embedded in the essentially undisturbed crystalline lithium niobate matrix. The optical waveguiding can be understood in terms of an average effective medium. With increasing depth, the track diameter become slightly larger following the increase of the electronic stopping power and the decrease of the amorphization threshold. The modified layer is therefore also characterized by a damage fraction and refractive index which increases with depth. Preliminary experiments suggest the application of such waveguides in the medium infrared range for astrophysics and other fields. The performance should be significantly better for wavelengths in the mid-infrared where both scattering (due to inhomogeneities) and absorption bands are known to be much weaker. The large thickness of the optical barrier should provide enough optical confinement. Certainly, the irradiated thickness could be easily decreased and tuned for realistic infrared applications in the wavelength range < 10 microns, either by decreasing the ion energy or by irradiating at an angle. This could decrease the total strain and would prevent breaking of the samples at higher fluences if these are required for specific tayloring of the index profile. Further work should be devoted to optimize the irradiation parameters (ion, energy, fluence, angle of irradiation) in order to tailor the refractive index profiles and to obtain higher refractive index jumps and better optical confinement.

Acknowledgements

We acknowledge funding from the Spain's MICINN projects MAT2005-06359 and MAT-2008-06794.

#118545 - $15.00 USD Received 13 Oct 2009; revised 30 Nov 2009; accepted 30 Nov 2009; published 18 Dec 2009